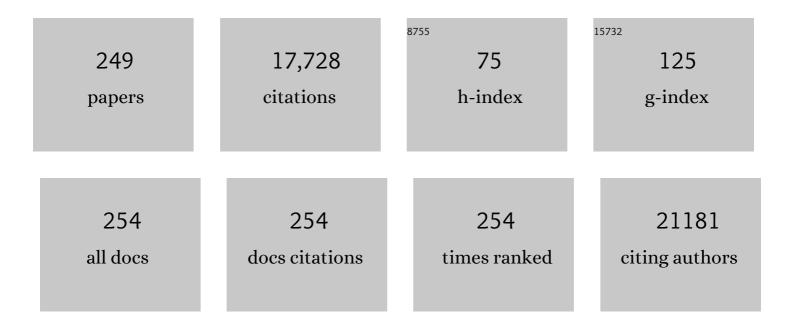
List of Publications by Year in descending order

Source: https://exaly.com/author-pdf/7311334/publications.pdf Version: 2024-02-01



#	Article	IF	CITATIONS
1	Highly Responsive Ultrathin GaS Nanosheet Photodetectors on Rigid and Flexible Substrates. Nano Letters, 2013, 13, 1649-1654.	9.1	683
2	Synthesis of Novel Thin-Film Materials by Pulsed Laser Deposition. Science, 1996, 273, 898-903.	12.6	547
3	PdSe ₂ : Pentagonal Two-Dimensional Layers with High Air Stability for Electronics. Journal of the American Chemical Society, 2017, 139, 14090-14097.	13.7	509
4	Nonlinear Fano-Resonant Dielectric Metasurfaces. Nano Letters, 2015, 15, 7388-7393.	9.1	474
5	Calcium as the Superior Coating Metal in Functionalization of Carbon Fullerenes for High-Capacity Hydrogen Storage. Physical Review Letters, 2008, 100, 206806.	7.8	391
6	Carbon Nanotubes and Related Nanomaterials: Critical Advances and Challenges for Synthesis toward Mainstream Commercial Applications. ACS Nano, 2018, 12, 11756-11784.	14.6	388
7	Fast intensified CD photography of YBa2Cu3O7â^'x laser ablation in vacuum and ambient oxygen. Applied Physics Letters, 1992, 60, 2732-2734.	3.3	383
8	Equally Efficient Interlayer Exciton Relaxation and Improved Absorption in Epitaxial and Nonepitaxial MoS ₂ /WS ₂ Heterostructures. Nano Letters, 2015, 15, 486-491.	9.1	337
9	Anisotropic Electron-Photon and Electron-Phonon Interactions in Black Phosphorus. Nano Letters, 2016, 16, 2260-2267.	9.1	328
10	Time-resolved imaging of gas phase nanoparticle synthesis by laser ablation. Applied Physics Letters, 1998, 72, 2987-2989.	3.3	318
11	In situ measurements and modeling of carbon nanotube array growth kinetics during chemical vapor deposition. Applied Physics A: Materials Science and Processing, 2005, 81, 223-240.	2.3	300
12	High-Performance Flexible Perovskite Solar Cells by Using a Combination of Ultrasonic Spray-Coating and Low Thermal Budget Photonic Curing. ACS Photonics, 2015, 2, 680-686.	6.6	268
13	Interlayer Coupling in Twisted WSe ₂ /WS ₂ Bilayer Heterostructures Revealed by Optical Spectroscopy. ACS Nano, 2016, 10, 6612-6622.	14.6	249
14	Perovskite Solar Cells with Near 100% Internal Quantum Efficiency Based on Large Single Crystalline Grains and Vertical Bulk Heterojunctions. Journal of the American Chemical Society, 2015, 137, 9210-9213.	13.7	246
15	Two-dimensional GaSe/MoSe ₂ misfit bilayer heterojunctions by van der Waals epitaxy. Science Advances, 2016, 2, e1501882.	10.3	239
16	Ultrathin nanosheets of CrSiTe ₃ : a semiconducting two-dimensional ferromagnetic material. Journal of Materials Chemistry C, 2016, 4, 315-322.	5.5	235
17	Controlled Vapor Phase Growth of Single Crystalline, Two-Dimensional GaSe Crystals with High Photoresponse. Scientific Reports, 2014, 4, 5497.	3.3	222
18	Patterned arrays of lateral heterojunctions within monolayer two-dimensional semiconductors. Nature Communications, 2015, 6, 7749.	12.8	213

#	Article	IF	CITATIONS
19	Dynamics of laser ablation plume penetration through low pressure background gases. Applied Physics Letters, 1995, 67, 197-199.	3.3	189
20	Low-Frequency Interlayer Breathing Modes in Few-Layer Black Phosphorus. Nano Letters, 2015, 15, 4080-4088.	9.1	182
21	In-Plane Optical Anisotropy of Layered Gallium Telluride. ACS Nano, 2016, 10, 8964-8972.	14.6	179
22	Low-Frequency Interlayer Raman Modes to Probe Interface of Twisted Bilayer MoS ₂ . Nano Letters, 2016, 16, 1435-1444.	9.1	177
23	Low Temperature Growth of Boron Nitride Nanotubes on Substrates. Nano Letters, 2005, 5, 2528-2532.	9.1	176
24	Nature of the band gap and origin of the electro-/photo-activity of Co3O4. Journal of Materials Chemistry C, 2013, 1, 4628.	5.5	176
25	Dynamics of Plume Propagation and Splitting during Pulsed-Laser Ablation. Physical Review Letters, 1997, 79, 1571-1574.	7.8	174
26	Structure and Formation Mechanism of Black TiO ₂ Nanoparticles. ACS Nano, 2015, 9, 10482-10488.	14.6	170
27	Physics and diagnostics of laser ablation plume propagation for high-Tc superconductor film growth. Thin Solid Films, 1992, 220, 138-145.	1.8	165
28	Fast and highly anisotropic thermal transport through vertically aligned carbon nanotube arrays. Applied Physics Letters, 2006, 89, 223110.	3.3	157
29	Near-Edge X-ray Absorption Fine Structure Spectroscopy as a Tool for Investigating Nanomaterials. Small, 2006, 2, 26-35.	10.0	152
30	Low-Frequency Raman Fingerprints of Two-Dimensional Metal Dichalcogenide Layer Stacking Configurations. ACS Nano, 2015, 9, 6333-6342.	14.6	151
31	Dynamics of single-wall carbon nanotube synthesis by laser vaporization. Applied Physics A: Materials Science and Processing, 2000, 70, 153-160.	2.3	148
32	Highly sensitive phototransistors based on two-dimensional GaTe nanosheets with direct bandgap. Nano Research, 2014, 7, 694-703.	10.4	140
33	Characterization of groundâ€state neutral and ion transport during laser ablation of Y1Ba2Cu3O7â^'xusing transient optical absorption spectroscopy. Applied Physics Letters, 1989, 55, 2345-2347.	3.3	137
34	Molecular Beam-Controlled Nucleation and Growth of Vertically Aligned Single-Wall Carbon Nanotube Arrays. Journal of Physical Chemistry B, 2005, 109, 16684-16694.	2.6	137
35	Low Energy Implantation into Transition-Metal Dichalcogenide Monolayers to Form Janus Structures. ACS Nano, 2020, 14, 3896-3906.	14.6	136
36	Characterization of thin-film amorphous semiconductors using spectroscopic ellipsometry. Thin Solid Films, 2000, 377-378, 68-73.	1.8	134

#	Article	IF	CITATIONS
37	Growth behavior of carbon nanotubes on multilayered metal catalyst film in chemical vapor deposition. Chemical Physics Letters, 2003, 374, 222-228.	2.6	133
38	Antioxidant Deactivation on Graphenic Nanocarbon Surfaces. Small, 2011, 7, 2775-2785.	10.0	133
39	Nucleation of Single-Walled Carbon Nanotubes. Physical Review Letters, 2003, 90, 145501.	7.8	127
40	In situ growth rate measurements and length control during chemical vapor deposition of vertically aligned multiwall carbon nanotubes. Applied Physics Letters, 2003, 83, 1851-1853.	3.3	127
41	Surface-Induced Orientation Control of CuPc Molecules for the Epitaxial Growth of Highly Ordered Organic Crystals on Graphene. Journal of the American Chemical Society, 2013, 135, 3680-3687.	13.7	125
42	Thickness-dependent charge transport in few-layer MoS ₂ field-effect transistors. Nanotechnology, 2016, 27, 165203.	2.6	124
43	High-Performance Field-Effect Transistors Based on Polystyrene- <i>b</i> -Poly(3-hexylthiophene) Diblock Copolymers. ACS Nano, 2011, 5, 3559-3567.	14.6	122
44	Tailoring Vacancies Far Beyond Intrinsic Levels Changes the Carrier Type and Optical Response in Monolayer MoSe _{2â^'<i>x</i>} Crystals. Nano Letters, 2016, 16, 5213-5220.	9.1	121
45	Twisted MoSe ₂ Bilayers with Variable Local Stacking and Interlayer Coupling Revealed by Low-Frequency Raman Spectroscopy. ACS Nano, 2016, 10, 2736-2744.	14.6	117
46	In situ imaging and spectroscopy of single-wall carbon nanotube synthesis by laser vaporization. Applied Physics Letters, 2000, 76, 182-184.	3.3	115
47	Carbon Nanotubes Grown on Metal Microelectrodes for the Detection of Dopamine. Analytical Chemistry, 2016, 88, 645-652.	6.5	113
48	Deep learning analysis of defect and phase evolution during electron beam-induced transformations in WS2. Npj Computational Materials, 2019, 5, .	8.7	113
49	In situ control of the catalyst efficiency in chemical vapor deposition of vertically aligned carbon nanotubes on predeposited metal catalyst films. Applied Physics Letters, 2004, 84, 1759-1761.	3.3	110
50	PSâ€ <i>b</i> â€₽3HT Copolymers as P3HT/PCBM Interfacial Compatibilizers for High Efficiency Photovoltaics. Advanced Materials, 2011, 23, 5529-5535.	21.0	110
51	Photoluminescence from gas-suspended SiOx nanoparticles synthesized by laser ablation. Applied Physics Letters, 1998, 73, 438-440.	3.3	108
52	Pulsed Laser Deposition of Photoresponsive Twoâ€Dimensional GaSe Nanosheet Networks. Advanced Functional Materials, 2014, 24, 6365-6371.	14.9	108
53	Excimer laser reduction and patterning of graphite oxide. Carbon, 2013, 53, 81-89.	10.3	107
54	Imaging of Vapor Plumes Produced by Matrix Assisted Laser Desorption: A Plume Sharpening Effect. Physical Review Letters, 1999, 83, 444-447.	7.8	103

#	Article	IF	CITATIONS
55	The isotopic effects of deuteration on optoelectronic properties of conducting polymers. Nature Communications, 2014, 5, 3180.	12.8	103
56	Van der Waals Epitaxial Growth of Two-Dimensional Single-Crystalline GaSe Domains on Graphene. ACS Nano, 2015, 9, 8078-8088.	14.6	103
57	Ultrafast Charge Transfer and Hybrid Exciton Formation in 2D/0D Heterostructures. Journal of the American Chemical Society, 2016, 138, 14713-14719.	13.7	102
58	In situ edge engineering in two-dimensional transition metal dichalcogenides. Nature Communications, 2018, 9, 2051.	12.8	100
59	Deciphering Halogen Competition in Organometallic Halide Perovskite Growth. Journal of the American Chemical Society, 2016, 138, 5028-5035.	13.7	92
60	Dynamics of plume propagation, splitting, and nanoparticle formation during pulsed-laser ablation. Applied Surface Science, 1998, 127-129, 151-158.	6.1	91
61	Directed Integration of Tetracyanoquinodimethane-Cu Organic Nanowires into Prefabricated Device Architectures. Advanced Materials, 2006, 18, 2184-2188.	21.0	91
62	Cooperative Island Growth of Large-Area Single-Crystal Graphene on Copper Using Chemical Vapor Deposition. ACS Nano, 2014, 8, 5657-5669.	14.6	91
63	Single-Crystal Organic Nanowires of Copper–Tetracyanoquinodimethane: Synthesis, Patterning, Characterization, and Device Applications. Angewandte Chemie - International Edition, 2007, 46, 2650-2654.	13.8	90
64	Formation of single crystalline ZnO nanotubes without catalysts and templates. Applied Physics Letters, 2007, 90, 113108.	3.3	89
65	Synthesis and emerging properties of 2D layered Ill–VI metal chalcogenides. Applied Physics Reviews, 2019, 6, 041312.	11.3	89
66	Rapid Growth of Long, Vertically Aligned Carbon Nanotubes through Efficient Catalyst Optimization Using Metal Film Gradients. Nano Letters, 2004, 4, 1939-1942.	9.1	88
67	Dynamics of plume propagation and splitting during pulsed-laser ablation of Si in He and Ar. Physical Review B, 1998, 58, 1533-1543.	3.2	87
68	Investigations of single-wall carbon nanotube growth by time-restricted laser vaporization. Physical Review B, 2002, 65, .	3.2	87
69	Imaging and blackbody emission spectra of particulates generated in the KrFâ€kaser ablation of BN and YBa2Cu3O7â^x. Applied Physics Letters, 1993, 62, 1463-1465.	3.3	86
70	Excitonic Dynamics in Janus MoSSe and WSSe Monolayers. Nano Letters, 2021, 21, 931-937.	9.1	86
71	Isoelectronic Tungsten Doping in Monolayer MoSe ₂ for Carrier Type Modulation. Advanced Materials, 2016, 28, 8240-8247.	21.0	85
72	Suppression of Defects and Deep Levels Using Isoelectronic Tungsten Substitution in Monolayer MoSe ₂ . Advanced Functional Materials, 2017, 27, 1603850.	14.9	84

5

#	Article	IF	CITATIONS
73	Metastable Copperâ€Phthalocyanine Singleâ€Crystal Nanowires and Their Use in Fabricating Highâ€Performance Fieldâ€Effect Transistors. Advanced Functional Materials, 2009, 19, 3776-3780.	14.9	81
74	Defect-Mediated Phase Transformation in Anisotropic Two-Dimensional PdSe ₂ Crystals for Seamless Electrical Contacts. Journal of the American Chemical Society, 2019, 141, 8928-8936.	13.7	81
75	Twoâ€Dimensional Palladium Diselenide with Strong Inâ€Plane Optical Anisotropy and High Mobility Grown by Chemical Vapor Deposition. Advanced Materials, 2020, 32, e1906238.	21.0	81
76	Enhancement of van der Waals Interlayer Coupling through Polar Janus MoSSe. Journal of the American Chemical Society, 2020, 142, 17499-17507.	13.7	80
77	A water-soluble polythiophene for organic field-effect transistors. Polymer Chemistry, 2013, 4, 5270.	3.9	78
78	Laser ablation plume thermalization dynamics in background gases: combined imaging, optical absorption and emission spectroscopy, and ion probe measurements. Applied Surface Science, 1996, 96-98, 131-138.	6.1	75
79	Gas-phase diagnostics and LIF-imaging of 3-hydroxypicolinic acid maldi-matrix plumes. Chemical Physics Letters, 1998, 286, 425-432.	2.6	74
80	Enhancing Ion Migration in Grain Boundaries of Hybrid Organic–Inorganic Perovskites by Chlorine. Advanced Functional Materials, 2017, 27, 1700749.	14.9	74
81	Structure and optical properties of amorphous diamond films prepared by ArF laser ablation as a function of carbon ion kinetic energy. Applied Physics Letters, 1998, 73, 2591-2593.	3.3	70
82	Metal-assisted hydrogen storage on Pt-decorated single-walled carbon nanohorns. Carbon, 2012, 50, 4953-4964.	10.3	69
83	Single walled carbon nanohorns as photothermal cancer agents. Lasers in Surgery and Medicine, 2011, 43, 43-51.	2.1	67
84	Edge-Controlled Growth and Etching of Two-Dimensional GaSe Monolayers. Journal of the American Chemical Society, 2017, 139, 482-491.	13.7	65
85	Improving Light Harvesting in Dye-Sensitized Solar Cells Using Hybrid Bimetallic Nanostructures. ACS Photonics, 2016, 3, 385-394.	6.6	64
86	Electronic transport imaging in a multiwire SnO2 chemical field-effect transistor device. Journal of Applied Physics, 2005, 98, 044503.	2.5	62
87	Real-time imaging of vertically aligned carbon nanotube array growth kinetics. Nanotechnology, 2008, 19, 055605.	2.6	61
88	Accelerated Expansion of Laser-Ablated Materials near a Solid Surface. Physical Review Letters, 1995, 75, 4706-4709.	7.8	60
89	Gas-phase nanoparticle formation and transport during pulsed laser deposition of Y1Ba2Cu3O7â^'d. Applied Physics Letters, 1999, 74, 3788-3790.	3.3	60
90	Realâ€Time Observation of Orderâ€Disorder Transformation of Organic Cations Induced Phase Transition and Anomalous Photoluminescence in Hybrid Perovskites. Advanced Materials, 2018, 30, e1705801.	21.0	60

DAVID B GEOHEGAN

#	Article	IF	CITATIONS
91	Anomalous interlayer vibrations in strongly coupled layered PdSe ₂ . 2D Materials, 2018, 5, 035016.	4.4	60
92	Model for Self-Assembly of Carbon Nanotubes from Acetylene Based on Real-Time Studies of Vertically Aligned Growth Kinetics. Journal of Physical Chemistry C, 2009, 113, 15484-15491.	3.1	59
93	Carbon nanotube effects on electroluminescence and photovoltaic response in conjugated polymers. Applied Physics Letters, 2005, 87, 263118.	3.3	57
94	The effect of annealing on the electrical and thermal transport properties of macroscopic bundles of long multi-wall carbon nanotubes. Physica B: Condensed Matter, 2007, 388, 326-330.	2.7	57
95	Selective Patterned Growth of Single rystal Ag–TCNQ Nanowires for Devices by Vapor–Solid Chemical Reaction. Advanced Functional Materials, 2008, 18, 3043-3048.	14.9	57
96	Separation of junction and bundle resistance in single wall carbon nanotube percolation networks by impedance spectroscopy. Applied Physics Letters, 2010, 97, .	3.3	56
97	In Vitro and in Vivo Studies of Single-Walled Carbon Nanohorns with Encapsulated Metallofullerenes and Exohedrally Functionalized Quantum Dots. Nano Letters, 2010, 10, 2843-2848.	9.1	56
98	Correlating high power conversion efficiency of PTB7:PC ₇₁ BM inverted organic solar cells with nanoscale structures. Nanoscale, 2015, 7, 15576-15583.	5.6	54
99	Observation of Nanoscale Morphological and Structural Degradation in Perovskite Solar Cells by in Situ TEM. ACS Applied Materials & Interfaces, 2016, 8, 32333-32340.	8.0	54
100	Simple model of the interrelation between single- and multiwall carbon nanotube growth rates for the CVD process. Physical Review B, 2007, 75, .	3.2	53
101	Electronâ€Beamâ€Related Studies of Halide Perovskites: Challenges and Opportunities. Advanced Energy Materials, 2020, 10, 1903191.	19.5	53
102	Condensed phase growth of single-wall carbon nanotubes from laser annealed nanoparticulates. Applied Physics Letters, 2001, 78, 3307-3309.	3.3	52
103	High Conduction Hopping Behavior Induced in Transition Metal Dichalcogenides by Percolating Defect Networks: Toward Atomically Thin Circuits. Advanced Functional Materials, 2017, 27, 1702829.	14.9	52
104	Controllable Thinâ€Film Approaches for Doping and Alloying Transition Metal Dichalcogenides Monolayers. Advanced Science, 2021, 8, 2004249.	11.2	51
105	Comparative diagnostics of ArF- and KrF-laser generated carbon plumes used for amorphous diamond-like carbon film deposition. Applied Surface Science, 1996, 96-98, 859-865.	6.1	50
106	Raman study of Fano interference in <i>p</i> â€ŧype doped silicon. Journal of Raman Spectroscopy, 2010, 41, 1759-1764.	2.5	49
107	Room-Temperature Electron–Hole Liquid in Monolayer MoS ₂ . ACS Nano, 2019, 13, 10351-10358.	14.6	49
108	Growth, Patterning, and One-Dimensional Electron -Transport Properties of Self-Assembled Ag-TCNQF4 Organic Nanowires. Chemistry of Materials, 2009, 21, 4275-4281.	6.7	48

#	Article	IF	CITATIONS
109	Modeling of dynamical processes in laser ablation. Applied Surface Science, 1996, 96-98, 14-23.	6.1	47
110	Digital Transfer Growth of Patterned 2D Metal Chalcogenides by Confined Nanoparticle Evaporation. ACS Nano, 2014, 8, 11567-11575.	14.6	47
111	Improving Dispersion of Single-Walled Carbon Nanotubes in a Polymer Matrix Using Specific Interactions. Chemistry of Materials, 2006, 18, 3513-3522.	6.7	46
112	Low thermal budget, photonic-cured compact TiO ₂ layers for high-efficiency perovskite solar cells. Journal of Materials Chemistry A, 2016, 4, 9685-9690.	10.3	46
113	Strain tolerance of two-dimensional crystal growth on curved surfaces. Science Advances, 2019, 5, eaav4028.	10.3	46
114	Revealing the Preferred Interlayer Orientations and Stackings of Twoâ€Dimensional Bilayer Gallium Selenide Crystals. Angewandte Chemie - International Edition, 2015, 54, 2712-2717.	13.8	45
115	Synthesis and characterization of single-wall carbon nanotube–amorphous diamond thin-film composites. Applied Physics Letters, 2002, 81, 2097-2099.	3.3	44
116	Observation of two distinct negative trions in tungsten disulfide monolayers. Physical Review B, 2015, 92, .	3.2	44
117	Ultrafast Spectral Dynamics of CsPb(Br _{<i>x</i>} Cl _{1–<i>x</i>}) ₃ Mixed-Halide Nanocrystals. ACS Photonics, 2018, 5, 3575-3583.	6.6	44
118	Nanoparticle generation and transport resulting from femtosecond laser ablation of ultrathin metal films: Time-resolved measurements and molecular dynamics simulations. Applied Physics Letters, 2014, 104, .	3.3	42
119	Ultrafast Dynamics of Metal Plasmons Induced by 2D Semiconductor Excitons in Hybrid Nanostructure Arrays. ACS Photonics, 2016, 3, 2389-2395.	6.6	42
120	lsotope-Engineering the Thermal Conductivity of Two-Dimensional MoS ₂ . ACS Nano, 2019, 13, 2481-2489.	14.6	42
121	Pulsed Growth of Vertically Aligned Nanotube Arrays with Variable Density. ACS Nano, 2010, 4, 7573-7581.	14.6	41
122	Controllable Growth of Perovskite Films by Roomâ€Temperature Air Exposure for Efficient Planar Heterojunction Photovoltaic Cells. Angewandte Chemie - International Edition, 2015, 54, 14862-14865.	13.8	41
123	Development of pulsed laser-assisted thermal relaxation technique for thermal characterization of microscale wires. Journal of Applied Physics, 2008, 103, .	2.5	40
124	Intrinsic Defects in MoS ₂ Grown by Pulsed Laser Deposition: From Monolayers to Bilayers. ACS Nano, 2021, 15, 2858-2868.	14.6	40
125	Modeling of plume dynamics in laser ablation processes for thin film deposition of materials. Physics of Plasmas, 1996, 3, 2203-2209.	1.9	39
126	Understanding How Processing Additives Tune the Nanoscale Morphology of High Efficiency Organic Photovoltaic Blends: From Casting Solution to Spun ast Thin Film. Advanced Functional Materials, 2014, 24, 6647-6657.	14.9	39

#	Article	IF	CITATIONS
127	Growth of highly doped pâ€ŧype ZnTe films by pulsed laser ablation in molecular nitrogen. Applied Physics Letters, 1995, 67, 2545-2547.	3.3	38
128	High-density vertically aligned multiwalled carbon nanotubes with tubular structures. Applied Physics Letters, 2005, 86, 253105.	3.3	38
129	Theory and numerical modeling of the accelerated expansion of laser-ablated materials near a solid surface. Physical Review B, 1999, 60, 8373-8382.	3.2	37
130	Ultrafast carrier dynamics in bimetallic nanostructure-enhanced methylammonium lead bromide perovskites. Nanoscale, 2017, 9, 1475-1483.	5.6	37
131	Laser-solid interaction and dynamics of laser-ablated materials. Applied Surface Science, 1996, 96-98, 45-49.	6.1	35
132	Cumulative and continuous laser vaporization synthesis of single wall carbon nanotubes and nanohorns. Applied Physics A: Materials Science and Processing, 2008, 93, 849-855.	2.3	34
133	The importance of chain connectivity in the formation of non-covalent interactions between polymers and single-walled carbon nanotubes and its impact on dispersion. Soft Matter, 2010, 6, 2801.	2.7	34
134	Flux-Dependent Growth Kinetics and Diameter Selectivity in Single-Wall Carbon Nanotube Arrays. ACS Nano, 2011, 5, 8311-8321.	14.6	33
135	Nonequilibrium Synthesis of TiO ₂ Nanoparticle "Building Blocks―for Crystal Growth by Sequential Attachment in Pulsed Laser Deposition. Nano Letters, 2017, 17, 4624-4633.	9.1	33
136	Mechanisms affecting kinetic energies of laserâ€ablated materials. Journal of Vacuum Science and Technology A: Vacuum, Surfaces and Films, 1996, 14, 1111-1114.	2.1	31
137	Mapping mesoscopic phase evolution during E-beam induced transformations via deep learning of atomically resolved images. Npj Computational Materials, 2018, 4, .	8.7	31
138	Characterization and Carbonization of Highly Oriented Poly(diiododiacetylene) Nanofibers. Macromolecules, 2011, 44, 2626-2631.	4.8	30
139	Low temperature synthesis of hierarchical TiO ₂ nanostructures for high performance perovskite solar cells by pulsed laser deposition. Physical Chemistry Chemical Physics, 2016, 18, 27067-27072.	2.8	29
140	Nonâ€Equilibrium Synthesis of Highly Active Nanostructured, Oxygenâ€Incorporated Amorphous Molybdenum Sulfide HER Electrocatalyst. Small, 2020, 16, e2004047.	10.0	29
141	Assembly of Single-Walled Carbon Nanohorn Supported Liposome Particles. Bioconjugate Chemistry, 2011, 22, 1012-1016.	3.6	28
142	Atomic Insight into Thermolysisâ€Driven Growth of 2D MoS ₂ . Advanced Functional Materials, 2019, 29, 1902149.	14.9	28
143	High-performance organic field-effect transistors with dielectric and active layers printed sequentially by ultrasonic spraying. Journal of Materials Chemistry C, 2013, 1, 4384.	5.5	27
144	Tilt Grain Boundary Topology Induced by Substrate Topography. ACS Nano, 2017, 11, 8612-8618.	14.6	27

#	Article	IF	CITATIONS
145	Time-resolved diagnostics of single wall carbon nanotube synthesis by laser vaporization. Applied Surface Science, 2002, 197-198, 552-562.	6.1	26
146	Species-resolved imaging and gated photon counting Spectroscopy of laser ablation plume dynamics During krf- and arf-laser pld of amorphous diamond films. Materials Research Society Symposia Proceedings, 1995, 397, 55.	0.1	25
147	Pulsed laser CVD investigations of single-wall carbon nanotube growth dynamics. Applied Physics A: Materials Science and Processing, 2008, 93, 987-993.	2.3	25
148	Investigation ofGd3N@C2nâ€,(40≤≤4)family by Raman and inelastic electron tunneling spectroscopy. Physical Review B, 2010, 81, .	3.2	25
149	Photocarrier Transfer across Monolayer MoS ₂ –MoSe ₂ Lateral Heterojunctions. ACS Nano, 2018, 12, 7086-7092.	14.6	25
150	Pulsed laser deposition of thin superconducting films of Ho ₁ Ba ₂ Cu ₃ O ₇ â^' <i>x</i> and Y ₁ Ba ₂ Cu ₃ O _{7 â^' <i>x</i> /sub>. Journal of Materials Research, 1988, 3, 1169-1179.}	2.6	24
151	LIF imaging and gas-phase diagnostics of laser desorbed MALDI-matrix plumes. Applied Surface Science, 1998, 127-129, 248-254.	6.1	24
152	Operation of individual integrally gated carbon nanotube field emitter cells. Applied Physics Letters, 2002, 81, 2860-2862.	3.3	24
153	Scanning probe microscopy imaging of frequency dependent electrical transport through carbon nanotube networks in polymers. Nanotechnology, 2004, 15, 907-912.	2.6	23
154	Fluorination of "brick and mortar―soft-templated graphitic ordered mesoporous carbons for high power lithium-ion battery. Journal of Materials Chemistry A, 2013, 1, 9414.	10.3	23
155	Uniform, Homogenous Coatings of Carbon Nanohorns on Arbitrary Substrates from Common Solvents. ACS Applied Materials & Interfaces, 2013, 5, 13153-13160.	8.0	23
156	Bottom up synthesis of boron-doped graphene for stable intermediate temperature fuel cell electrodes. Carbon, 2017, 123, 605-615.	10.3	23
157	Ultrafast Exciton Dissociation at the 2D-WS ₂ Monolayer/Perovskite Interface. Journal of Physical Chemistry C, 2018, 122, 28910-28917.	3.1	23
158	One-dimensional electron transport in Cu-tetracyanoquinodimethane organic nanowires. Applied Physics Letters, 2007, 90, 193115.	3.3	22
159	A Facile High-speed Vibration Milling Method to Water-disperse Single-walled Carbon Nanohorns. Chemistry of Materials, 2010, 22, 347-351.	6.7	22
160	Real-time optical diagnostics of graphene growth induced by pulsed chemical vapor deposition. Nanoscale, 2013, 5, 6507.	5.6	22
161	Absorption spectrum of Kr2F(4 2Γ) in the near ultraviolet and visible (335â‰͡¤â‰@00 nm): Comparison wit Kr+2(1(1/2)u) measurements. Journal of Chemical Physics, 1988, 89, 3410-3427.	h 3.0	21
162	Bromine substitution improves excited-state dynamics in mesoporous mixed halide perovskite films. Nanoscale, 2017, 9, 12005-12013.	5.6	21

10

#	Article	IF	CITATIONS
163	The growth and assembly of organic molecules and inorganic 2D materials on graphene for van der Waals heterostructures. Carbon, 2018, 131, 246-257.	10.3	21
164	Photon ontrolled fabrication of amorphous superlattice structures using ArF (193 nm) excimer laser photolysis. Applied Physics Letters, 1988, 52, 1868-1870.	3.3	20
165	Structural control of vertically aligned multiwalled carbon nanotubes by radio-frequency plasmas. Applied Physics Letters, 2005, 87, 173106.	3.3	20
166	A laser-deposition approach to compositional-spread discovery of materials on conventional sample sizes. Measurement Science and Technology, 2005, 16, 21-31.	2.6	20
167	Imperfect surface order and functionalization in vertical carbon nanotube arrays probed by near edge X-ray absorption fine structure spectroscopy (NEXAFS). Physical Chemistry Chemical Physics, 2006, 8, 5038.	2.8	20
168	THERMAL CHARACTERIZATION OF MULTI-WALL CARBON NANOTUBE BUNDLES BASED ON PULSED LASER-ASSISTED THERMAL RELAXATION. Functional Materials Letters, 2008, 01, 71-76.	1.2	20
169	Persistent photoconductivity in two-dimensional Mo _{1â^'<i>x</i>} W _{<i>x</i>} Se ₂ –MoSe ₂ van der Waals heterojunctions. Journal of Materials Research, 2016, 31, 923-930.	2.6	20
170	Column IIIA metal film deposition by dissociative photoionization of metal halide vapors. Applied Physics Letters, 1984, 45, 1146-1148.	3.3	19
171	Integrally gated carbon nanotube field emission cathodes produced by standard microfabrication techniques. Journal of Vacuum Science & Technology an Official Journal of the American Vacuum Society B, Microelectronics Processing and Phenomena, 2003, 21, 957.	1.6	19
172	Formation studies and controlled production of carbon nanohorns using continuousin situcharacterization techniques. Nanotechnology, 2007, 18, 185604.	2.6	19
173	Strain-Induced Growth of Twisted Bilayers during the Coalescence of Monolayer MoS ₂ Crystals. ACS Nano, 2021, 15, 4504-4517.	14.6	19
174	The electrodeposition of metal at metal/carbon nanotube junctions. Chemical Physics Letters, 2002, 361, 525-529.	2.6	18
175	In situ timeâ€resolved measurements of carbon nanotube and nanohorn growth. Physica Status Solidi (B): Basic Research, 2007, 244, 3944-3949.	1.5	18
176	Janus Monolayers for Ultrafast and Directional Charge Transfer in Transition Metal Dichalcogenide Heterostructures. ACS Nano, 2022, 16, 4197-4205.	14.6	18
177	Resonantly enhanced three-photon ionization of krypton. Physical Review A, 1986, 33, 269-275.	2.5	17
178	Epitaxial growth of Ge films on GaAs (285–415 °C) by laser photochemical vapor deposition. Applied Physics Letters, 1988, 52, 1710-1712.	3.3	17
179	Understanding the Metal-Directed Growth of Single-Crystal M-TCNQF ₄ Organic Nanowires with Time-Resolved, in Situ X-ray Diffraction and First-Principles Theoretical Studies. Journal of the American Chemical Society, 2012, 134, 14353-14361.	13.7	17
180	Revealing the surface and bulk regimes of isothermal graphene nucleation and growth on Ni with in situ kinetic measurements and modeling. Carbon, 2014, 79, 256-264.	10.3	16

#	Article	IF	CITATIONS
181	Spatial Mapping of Thermal Boundary Conductance at Metal–Molybdenum Diselenide Interfaces. ACS Applied Materials & Interfaces, 2019, 11, 14418-14426.	8.0	16
182	ArF laser photochemical deposition of amorphous silicon from disilane: Spectroscopic studies and comparison with thermal CVD. Applied Surface Science, 1989, 36, 70-80.	6.1	15
183	Fast-Iccd Photography and Gated Photon Counting Measurements of Blackbody Emission from Particulates Generated in The KrF-Laser Ablation of BN and YBCO. Materials Research Society Symposia Proceedings, 1992, 285, 27. Vibrational Spectrum of the endohedral <mml:math< td=""><td>0.1</td><td>15</td></mml:math<>	0.1	15
184	xmlns:mml="http://www.w3.org/1998/Math/MathML" display="inline"> <mml:mrow><mml:msub><mml:mi mathvariant="normal">Y<mml:mrow><mml:mn>2</mml:mn></mml:mrow></mml:mi </mml:msub></mml:mrow> xmlns:mml="http://www.w3.org/1998/Math/MathML" display="inline"> <mml:mrow><mml:msub><td>> {/mml:m 3.2</td><td>hath>C<mml< td=""></mml<></td></mml:msub></mml:mrow>	> {/mml:m 3.2	hath>C <mml< td=""></mml<>
185	Asplay= Inine >2 <td>8.0</td> <td>15</td>	8.0	15
186	Absorption of electronically excited Xe2Cl in the ultraviolet. Journal of Chemical Physics, 1985, 82, 4862-4866.	3.0	14
187	Spatial and temporal measurements of temperature and cell viability in response to nanoparticle-mediated photothermal therapy. Nanomedicine, 2012, 7, 1729-1742.	3.3	14
188	In situ laser reflectivity to monitor and control the nucleation and growth of atomically thin 2D materials*. 2D Materials, 2020, 7, 025048.	4.4	14
189	Selective Antisite Defect Formation in WS ₂ Monolayers via Reactive Growth on Dilute Wâ€Au Alloy Substrates. Advanced Materials, 2022, 34, e2106674.	21.0	14
190	Stabilized Synthesis of 2D Verbeekite: Monoclinic PdSe ₂ Crystals with High Mobility and In-Plane Optical and Electrical Anisotropy. ACS Nano, 2022, 16, 13900-13910.	14.6	14
191	Xe2Cl and Kr2F excited state (4 2Γ) absorption spectra: measurements of absolute cross sections. Chemical Physics Letters, 1987, 139, 519-524.	2.6	13
192	Low temperature photon-controlled growth of thin films and multilayered structures. Applied Surface Science, 1989, 36, 59-69.	6.1	12
193	In situ electric-field-induced contrast imaging of electronic transport pathways in nanotube-polymer composites. Applied Physics Letters, 2006, 89, 013114.	3.3	12
194	Nanostructured carbon electrocatalyst supports for intermediate-temperature fuel cells: Single-walled versus multi-walled structures. Journal of Power Sources, 2017, 337, 145-151.	7.8	12
195	Giant enhancement of exciton diffusivity in two-dimensional semiconductors. Science Advances, 2020, 6, .	10.3	12
196	Photoionization of vapor phase thallium and indium monohalides in the ultraviolet: Absolute cross sections and photofragment spectroscopy by photodetachment of lâ^'. Journal of Chemical Physics, 1984, 81, 5336-5351.	3.0	10
197	Heteroepitaxial growth of Ge films on (100) GaAs by pyrolysis of digermane. Applied Physics Letters, 1989, 55, 858-860.	3.3	10
198	Reorientation of carbon nanotubes in polymer matrix composites using compressive loading. Journal of Materials Research, 2005, 20, 1026-1032.	2.6	10

#	Article	IF	CITATIONS
199	High-temperature transformation of Fe-decorated single-wall carbon nanohorns to nanooysters: a combined experimental and theoretical study. Nanoscale, 2013, 5, 1849-1857.	5.6	10
200	Nanoscale Silicon as a Catalyst for Graphene Growth: Mechanistic Insight from <i>in Situ</i> Raman Spectroscopy. Journal of Physical Chemistry C, 2016, 120, 14180-14186.	3.1	10
201	Ultrafast Excited-State Dynamics in Shape- and Composition-Controlled Gold–Silver Bimetallic Nanostructures. Journal of Physical Chemistry C, 2017, 121, 4540-4547.	3.1	10
202	Incremental Growth of Short SWNT Arrays by Pulsed Chemical Vapor Deposition. Small, 2012, 8, 1534-1542.	10.0	9
203	Effect of purity on the electro-optical properties of single wall nanotube-based transparent conductive electrodes. Carbon, 2013, 64, 1-5.	10.3	9
204	Comment on "Single Crystals of Single-Walled Carbon Nanotubes Formed by Self-Assembly". Science, 2003, 300, 1236b-1236.	12.6	8
205	Altering the catalytic activity of thin metal catalyst films forÂcontrolled growth of chemical vapor deposited vertically aligned carbon nanotube arrays. Applied Physics A: Materials Science and Processing, 2008, 93, 1005-1009.	2.3	8
206	Narrow and intense resonances in the low-frequency region of surface-enhanced Raman spectra of single-wall carbon nanotubes. Physical Review B, 2010, 82, .	3.2	8
207	Heterogeneities at multiple length scales in 2D layered materials: From localized defects and dopants to mesoscopic heterostructures. Nano Research, 2021, 14, 1625-1649.	10.4	8
208	Absolute photoionization cross sections for Kr(5s) and Kr2 5s 3Σ+u (1u, 0â^'u) excited states at 248 nm Journal of Chemical Physics, 1987, 86, 577-587.	^{1.} 3.0	7
209	How the shape of catalyst nanoparticles determines their crystallographic orientation during carbon nanofiber growth. Carbon, 2013, 60, 41-45.	10.3	7
210	Cooperative Behavior in the Evolution of Alignment and Structure in Vertically Aligned Carbon-Nanotube Arrays Grown using Chemical Vapor Deposition. Physical Review Applied, 2018, 10, .	3.8	7
211	Understanding Substrate-Guided Assembly in van der Waals Epitaxy by <i>in Situ</i> Laser Crystallization within a Transmission Electron Microscope. ACS Nano, 2021, 15, 8638-8652.	14.6	7
212	Spectroscopic and Ion Probe Characterization of the Transport Process Following Laser Ablation of Yba ₂ Cu ₃ O _x . Materials Research Society Symposia Proceedings, 1990, 191, 211.	0.1	6
213	Slowing of femtosecond laser-generated nanoparticles in a background gas. Applied Physics Letters, 2014, 105, 213108.	3.3	6
214	Revealing the Preferred Interlayer Orientations and Stackings of Twoâ€Dimensional Bilayer Gallium Selenide Crystals. Angewandte Chemie, 2015, 127, 2750-2755.	2.0	5
215	A hybrid optimization algorithm to explore atomic configurations of TiO2 nanoparticles. Computational Materials Science, 2018, 141, 1-9.	3.0	4
216	Laser Interactions for the Synthesis and In Situ Diagnostics of Nanomaterials. Springer Series in Materials Science, 2014, , 143-173.	0.6	4

DAVID B GEOHEGAN

#	Article	IF	CITATIONS
217	Gated ICCD Photography of the KrF-Laser Ablation of Graphite into Background Gases. , 1994, , 349-354.		4
218	<title>Dynamics of the vapor plumes produced by the MALDI technique</title> . , 2000, 4070, 166.		3
219	Laser Interactions in Nanomaterials Synthesis. Springer Series in Materials Science, 2010, , 1-17.	0.6	3
220	LASER-BASED SYNTHESIS, DIAGNOSTICS, AND CONTROL OF SINGLE-WALLED CARBON NANOTUBES AND NANOHORNS FOR COMPOSITES AND BIOLOGICAL NANOVECTORS. , 2006, , 205-223.		3
221	XeCl laser power enhancement with an external ultraviolet laser. IEEE Journal of Quantum Electronics, 1986, 22, 501-504.	1.9	2
222	Collisional Effects of Background Gases on Pulsed Laser Deposition Plasma Beams. Materials Research Society Symposia Proceedings, 1995, 388, 21.	0.1	2
223	Fabrication of Ag-tetracyanoquinodimethane nanostructures using ink-jet printing/vapor-solid chemical reaction process. Journal of Vacuum Science & Technology B, 2008, 26, L48-L52.	1.3	2
224	<title>Pulsed-laser-deposited amorphous diamond and related materials: synthesis, characterization, and field emission properties</title> . , 1999, , .		1
225	<title>Crystallinities and light-emitting properties of nanostructured SiGe alloy prepared by pulsed laser ablation in inert background gases</title> . , 1999, 3618, 512.		1
226	<title>In-situ plasma diagnostic investigations of single-wall carbon nanotube synthesis by laser
ablation of C-Ni-Co targets</title> . , 2000, , .		1
227	Synthesis of multifunctional single-wall carbon nanotube-amorphous diamond thin film composites. , 2003, , .		1
228	Laser Synthesis, Processing, and Spectroscopy of Atomically-Thin Two Dimensional Materials. Springer Series in Materials Science, 2018, , 1-37.	0.6	1
229	Signature of Many-Body Localization of Phonons in Strongly Disordered Superlattices. Nano Letters, 2021, 21, 7419-7425.	9.1	1
230	Nonequilibrium synthesis and processing approaches to tailor heterogeneity in 2D materials. , 2022, , 221-258.		1
231	Laser synthesis and processing of atomically thin 2D materials. Trends in Chemistry, 2022, 4, 769-772.	8.5	1
232	Radiative collision-induced electron continuum-continuum scattering. Physical Review A, 1983, 28, 1395-1400.	2.5	0
233	Doubleâ€exposure speckle photography for the measurement of small displacements. American Journal of Physics, 1983, 51, 315-320.	0.7	0
234	Modeling and simulation of short-channel MOSFETs operating in deep weak inversion. , 0, , .		0

14

#	Article	IF	CITATIONS
235	<title>Computer modeling of the interaction of a laser-ablated plume with an ambient background gas</title> . , 2000, , .		0
236	<title>Aspects of nanoparticle formation during pulsed laser ablation</title> ., 2000, , .		0
237	Time-resolved diagnostics and mechanisms of single-wall carbon nanotube synthesis by the laser vaporization technique. , 2001, , .		0
238	<title>Laser synthesis of single-wall carbon nanotubes with time-resolved in-situ diagnostics</title> . , 2002, , .		0
239	<title>Laser synthesis of single-wall carbon nanotubes with time-resolved in situ diagnostics</title> . , 2002, 4762, 268.		0
240	In situ optical absorption spectroscopy, incandencence, and light-scattering characterization of single-wall carbon nanotube synthesis by the laser vaporization technique. , 2003, 4977, 648.		0
241	Nonequilibrium laser synthesis and real-time diagnostics of carbon nanomaterial growth. , 2012, , .		0
242	New approaches for synthesis and processing of 2D materials (Conference Presentation). , 2017, , .		0
243	Pulsed laser vaporization synthesis of boron loaded few layered graphene (Conference Presentation). , 2017, , .		0
244	Optical signatures of defects in low temperature Raman and photoluminescence spectra of 2D crystals (Conference Presentation). , 2017, , .		0
245	Ultrafast charge and energy exchanges at hybrid interfaces involving 2D semiconductors (Conference) Tj ETQq1 1	0.7843	14 rgBT /Over
246	Correlating the optical properties of WS2 monolayers grown by CVD with isoelectronic Mo doping level (Conference Presentation). , 2017, , .		0
247	In Situ X-Ray Studies of Crystallization Kinetics and Ordering in Functional Organic and Hybrid Materials. , 2018, , 33-60.		0
248	Laser-synthesis of single-wall carbon nanotubes with time-resolved in situ diagnostics. , 2001, , .		0
249	Laser ablation plume thermalization dynamics in background gases: combined imaging, optical absorption and emission spectroscopy, and ion probe measurements. , 1996, , 131-138.		Ο